Use of a Biodegradable Material to Manufacture a Plansifter Suspension System

VIRGIL TUDOSE[1]*, RADU FRANCISC COTERLICI[2], DANIELA IOANA TUDOSE[1], ALEXANDRA HADAR[3], GABRIEL ALEXANDRU CONSTANTIN[4]

[1] Politehnica University of Bucharest, Faculty of Engineering and Management of Technological Systems, 060042, 313 Splaiul Independentei, Bucharest, Romania

[2] Transilvania University, Faculty of Materials Sciences and Engineering, 29 Eroilor Blvd., 500036, Brasov, Romania

[3] Politehnica University of Bucharest, Faculty of Entrepreuneurship, Business Engineering and Management, 313 Splaiul Independentei, 060042, Bucharest, Romania

[4] Politehnica University of Bucharest, Faculty of Biotechnical Systems Engineering, 313 Splaiul Independenei, 060042, Bucharest, Romania

In this paper is presented an experimental, theoretical and numerical study about the use of a biodegradable composite material in the manufacturing process of the suspension elements for plane sieves used in mills from bakery industry. The material was obtained by reinforcing an unsaturated polyester resin with cotton fabric. Tensile tests were performed for materials having one, three, five and seven layers of cotton fabric and the optimum solution was chosen. The material properties, obtained from the experimental tests, were used in a finite element model realized for the strength calculus of the suspension element. The numerical results were validated analytically. The study confirms that the biodegradable materials can be used for manufacturing of the suspension elements of a plansifter and can be adapted for other parts or industrial structures.

Keywords: sifting, biodegradable material, polyester resin, finite element, cotton

A plansifter consist of a number of compartments containing overlapping sifting surfaces, under roto-translation motion induced by a vertical shaft with counterweights. During service, a certain point of the machine describes a circle in a horizontal plane, the radius of the circle being the amplitude of movement [1]. In the dynamics of the sifting process such machines, which was analysed for the first time by Jansen and Glastonbury [2] and recently by Liu [3], an influence factor is the suspension system. An example of a plansifter is presented in figure 1, were one can see the suspension elements grouped into four sets of eight elements.

Fig. 1. Plansifter with eight compartments (4 x 2, placed back to back) [4]

The elements of the suspension system have lengths between 1.5 and 2.5 m, circular cross-section and can be manufactured from boiled beech wood, bamboo, steel, plastic material reinforced with carbon fibres. During service, they are subject to traction (due to the mass that they are supporting), bending and shear (due to the movement in the horizontal plane of the plansifter). If the bending stiffness of the supports decreases, then the amplitude of the plansifter increases, influencing thus the sifting process [5].

The conditions and standards required in the food industry motivate researches to use ecological and biodegradable materials. In order to have a biodegradable character, a synthetic material must be reinforced with natural fibres (cotton, hemp, flax, sisal, bamboo). The characteristics of a material depend on the properties of its constituents, on their distribution and on the way how they interact [6]. Generally, natural fibres have mechanical properties comparable to those of glass fibre or carbon and low specific weight, they are widespread in nature and have a low cost [7-9].

In engineering, cotton is often used for reinforcement of composite materials, in the form of fabric or short fibres. If the reinforcement is made with fabric, the mechanical strength of the composite increases with the percentage of cotton [10-11]. Pamuk et al. [12] have studied the traction, compression and impact behaviour of an epoxy resin reinforced with flax or cotton fibres in the form of fabric and have obtained mechanical properties superior to the ones of the resin. Due to their properties, composite materials reinforced with natural fibres have varied application areas, being used to manufacture different structures from simple packaging to components in the automotive industry [13-14].

In this paper, tensile tests have been performed for a polyester resin reinforced with one, three, five and seven layers of cotton fabric. Since the highest tensile strength was obtained for the material with five layers, the possibility to manufacture plansifter suspension elements from such material was investigated. For this purpose, a finite element model was built, having the mechanical

* *email: virgil.tudose@upb.roTel.: 0727353867*

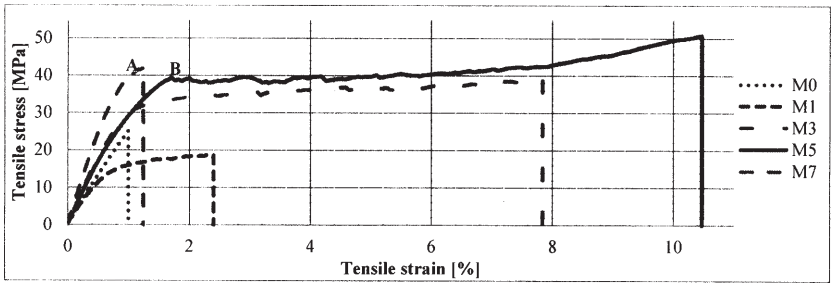

Fig. 2. Characteristic curves obtained for the five materials

characteristics of the material with five layers of cotton, obtained from mechanical tests. Two calculations were performed with the finite element method: one in which it was considered that the material is linear elastic and another in which non-linearity was taken into consideration by introducing the experimental stress-strain curve. The obtained results were confirmed by analytical calculations and have shown maximum stresses obtained numerically are far below the ultimate stress of the proposed material.

Experimental part

In order to determine the optimum number of layers of cotton fabric used to reinforce the polyester resin (Nestrapol 450-66), the mechanical properties obtained from tensile tests for five materials, with zero, one, three, five and seven layers of fabric were studied. The materials were obtained as plates, by manual casting of resin alternatively between the layers of cotton fabric. Material was left for hardening seven days, at a temperature of 20°C. Five specimens from each material were manufactured, according to the standard ISO 527-1 (2000) [15]. The characteristics of each specimen are listed in table 1.

Table 1
CHARACTERISTICS OF THE SPECIMENS

Material	No. of fabric layers	Length L [mm]	Width b [mm]	Thickness h [mm]
M0	0	250	23.5	2.5
M1	1	250	23.5	1
M3	3	250	23.5	1.5
M5	5	250	23.5	2.5
M7	7	250	23.5	2.5

The tests were performed with an INSTRON 8800 testing machine, at a temperature of 20°C, with a loading rate of 1 mm/min. The curves obtained for the five materials are plotted in figure 2. In table 2 the main mechanical properties of the studied materials are presented.

It can be noticed that material M5 has the highest tensile strength but the stress values for which the resin fails is about the same as in the case of material M7 (see points A and B on the two curves). In practice, additional costs appear when a greater number of layers of fabric is introduced in the material. For this reason, the characteristics obtained for the material M5 were considered in the following calculations.

An important aspect is that the ultimate tensile strength of the material M1 is smaller than the one for simple resin (M0). This can be explained by the fact that the specimens made of the material M1 had a low thickness (1 mm) and the resin has been weakened by the insertion of cotton.

Table 2
MECHANICAL PROPERTIES OF THE MATERIALS

Material	Ultimate tensile strength [MPa]	Young's modulus [MPa]	Maximum strain [%]
M0	25.1	3376	1.02
M1	18.5	3433	2.43
M3	39.8	4080	7.84
M5	50.7	4270	10.47
M7	42.0	5551	1.25

Analytical calculation

The sifting efficiency of a plansifter is influenced by the amplitude of its motion. The amplitude depends on the stiffness of the plansifter suspension system. If an optimum value of the amplitude is established, then, knowing the bending stiffness of one suspension element, one can calculate the force acting on the fastening system. Obviously, this force is equal to the force with which the suspension elements act on the plansifter, and implicitly on the actuating mechanism.

A theoretical model for the calculation of the bending stiffness of a suspension element is shown in figure 3a. In figure 3b, the loads acting on the suspension element, and reactions of connecting parts are depicted.

Through its clamping, the upper end has all degrees of freedom constrained and, for the lower end, only the rotations in the longitudinal plane of the bar are blocked. The displacement of the lower end of the bar denoted as „u", represents the amplitude of motion and is equal to the radius of the circle described by this point during functioning. Because the rotations of the heads with respect to the longitudinal axis are blocked, the bending load in the plane (x,z) of the bar is a fully reversed one. For reasons of symmetry, calculation was performed only in the plane (x,z), being the same for any other longitudinal plane of the bar.

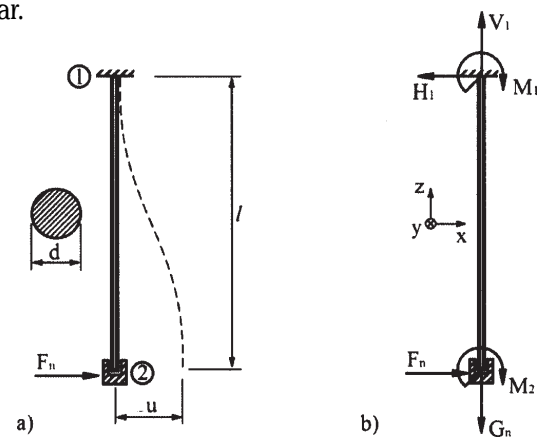

Fig. 3. The calculation model (a) and loads during service (b)

In figure 3b, the following notations have been considered: n – number of elastic supports of the plansifter; F_n – the force developed by one support on the plansifter, at its displacement equal to „u"; V_1, H_1, M_1 – reactions introduced by blocking the movements of the upper end; M_2 – reaction entered into the system by blocking the rotation of the lower end; G_n – the weight that an element must carry.

The relationship between the force F_n and u is written as:

$$F_n = k \cdot u,$$

where k is the stiffness during bending of the bar with a force F_n. Constantin et al. [16] determined the constant k for a similar model. Its expression is:

$$k = \frac{12EI}{l^3},$$

where E is Young's modulus of the bar material and I is the moment of inertia of the section about the axis perpendicular to the bending plane (axis y in this case).

One can calculate the acting force of the entire suspension system on the sieve as:

$$F = n \cdot F_n = n \cdot \frac{12EI}{l^3} \cdot u\,.$$

For the strength calculation of a support, it is necessary to know the reactions forces in the supports. Using the displacement method, a moment $M_2 = 0.5F_n \cdot l$, is obtained [17]. From the equilibrium equations, the other reactions are obtained. The diagrams of variation of the efforts that occur in the suspension element, along the z axis, are presented in figure 4. From these diagrams, one can notice that the maximum values are in sections 1 and 2. The maximum equivalent stresses in the two sections have the same values but are recorded in different points. In any point of the bar, the force F_n creates a shear stress (τ_{zx}), G_n and M_y produce normal stresses (σ_z), which can be cumulated.

For the numerical calculation, the parameters are replaced with the ones for the considered plansifter model. In the case of plansifter SPP 420, of Romanian production, the following parameters are known: total weight of the plansifter and its load (G) – 2155 kg; l – 1450 mm; u – 45 mm; d – 12 mm; n – 32 elastic supports.

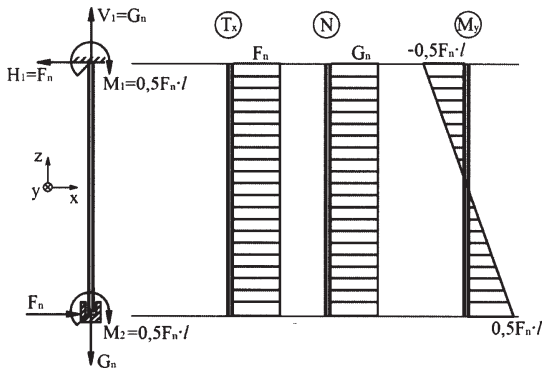

Fig. 4. Variation of the efforts for one suspension element

If the supports are made of the material proposed in this paper, a Young's modulus of 4270 MPa can be considered, in a linear elastic model. Substituting, one obtains:

$$F_n = \frac{12EI}{l^3} \cdot u = \frac{12 \cdot 4270 \cdot \frac{\pi 12^4}{64}}{1450^3} \cdot 45 = 0.770\ N;$$

$$G_n = \frac{G}{n} = \frac{2155 \cdot 9.81}{32} = 660.6\ N;$$

In figure 5a, the points in section 1 where the extreme values for stress σ_z appear are represented. Between the two points, the stress has a linear variation, as it is shown in figure 5b. Using relations from Strength of Materials, the following values were obtained for σ_z in point L (σ_z^L) and in point R (σ_z^R).

$$\sigma_z^L = \sigma_{z(b)}^L + \sigma_{z(t)}^L = \frac{-0.5F_n l}{\frac{\pi d^4}{64}} x_L + \frac{G_n}{A} =$$

$$= \frac{-0.5 \cdot 0.77 \cdot 1450}{\frac{\pi 12^4}{64}} (-6) + \frac{660.6}{\pi \cdot 6^2} = 9.132\ MPa;$$

$$\sigma_z^R = \sigma_{z(b)}^R + \sigma_{z(t)}^R = \frac{-0.5F_n l}{\frac{\pi d^4}{64}} x_R + \frac{G_n}{A} =$$

$$= \frac{-0.5 \cdot 0.77 \cdot 1450}{\frac{\pi 12^4}{64}} \cdot 6 + \frac{660.6}{\pi \cdot 6^2} = 2.55\ MPa,$$

where:

indices „b" and „t" correspond to bending and tensile stresses;

x_L and x_R are the coordinates on the x axis of points L and R;

A represents the cross section area of the bar.

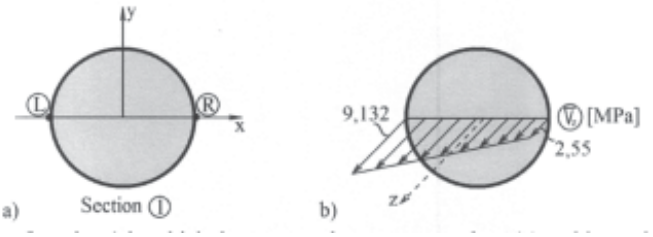

Fig. 5. Points of section 1 in which the stress σ_z has extreme values (a) and its variation in the direction defined by the two points (b)

The stress τ_{zx} in the two points is null and its maximum value (in the centroid of the cross section), calculated using the relation of Juravski [18], is much lower than the values obtained for σ_z. For this reason, the shear stress can be neglected. The maximum equivalent stress in the structure, obtained analytically, is in the point L of section 1 and has the value:

$$\sigma_{ech}^{max} = \sigma_z^L = 9.132\ MPa.$$

Numerical analysis

In order to present a numerical model for the suspension systems of a plansifter, a finite element analysis was carried out for the practical example studied analytically (the SPP 420 plansifter). Data from theoretical calculations were used to build the finite element models. To validate the numerical results, the displacement of the lower end of the suspension element was calculated and the result was compared to the analytical one.

Two calculations were performed, using the finite element program ANSYS: one in which the material of the suspension elements (M5) is linear elastic and another in which the real stress-strain curve, obtained from tensile tests was taken into consideration.

The geometry, boundary conditions and loading were the same in both cases and are shown in figure 6. To block the rotation of lower end of the suspension elements, two such elements, were modelled and connected through a body made of a more rigid material, with the Young's modulus E = $2 \cdot 10^6$ MPa. All degrees of freedom in the upper end were constrained.

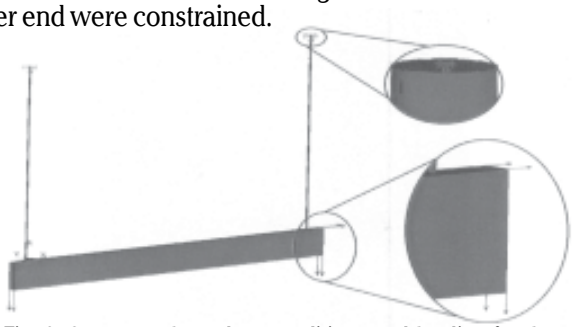

Fig. 6. Geometry, boundary conditions and loading for the two models

Fig. 7. Mesh of the two models

Loading consisted of four forces in the longitudinal direction of the elements (z axis of the model) and four forces in their transverse direction (x axis), applied in the corners of rigid body to preserve the model symmetry. Each of the forces on the z-axis direction is equal to $0.5G_n$ (330.3 N) and each of the other forces has a value of $0.5F_n$ (0.385 N).

The mesh with SOLID 186 elements [19], was the same for both models and is shown in figure 7.

For the linear elastic model, the elastic constants were considered E = 4270 MPa and ν =- 0.3. For the non-linear analysis, the characteristic curve of the material M5 from figure 2 was schematized by considering 12 intervals on which the material is considered linear, defined by 13 points. The obtained curve is shown in figure 8 and was inserted in the numerical model. The slope of the first interval is equal to 4270 MPa, the value considered in the linear elastic analysis (represented by the dashed line in fig. 8).

In figure 9a is shown the displacement field on the direction of the x axis obtained using the linear elastic

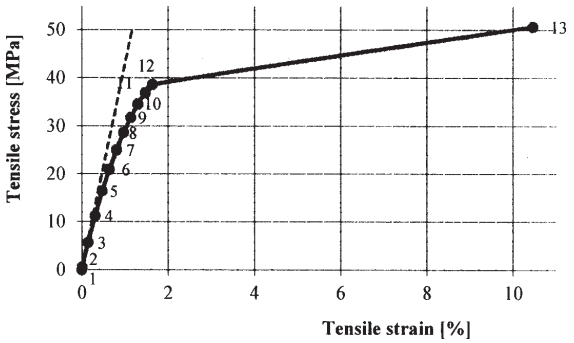

Fig. 8. Schematized characteristic curve of material M5

model while in figure 9b the same field is shown in the case of the nonlinear calculus. To validate the model, the value of the maximum displacement obtained for the first model is compared to the one imposed in the theoretical study, where the material was considered linear elastic. One can notice that the two values are very close (45 mm), and thus the numerical model is validated.

In figure 10 is presented the normal stresses field on the z axis for the linear elastic model. For the non-linear model, the results for σ_z are presented in figure 11.

In order to compare the analytical results with the numerical ones, the values of the stress σ_z were extracted in the nodes lying in the top section of one of the bars, illustrated in figure 12. These nodes are found in the direction defined by the points L and R from figure 5a. In figure 13 is represented the variation of the stress σ_z for all three calculations: analytical, numerical - linear and numerical - nonlinear. The coordinate which defines the position of a point is the one measured on the x axis from the system shown in figure 5a.

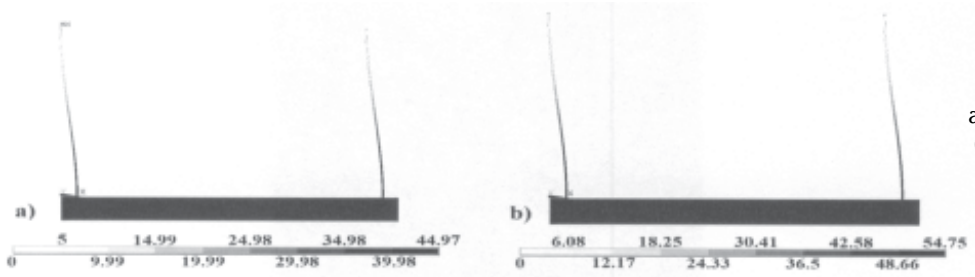

Fig. 9. Displacements field on the x axis [mm] obtained for linear analysis (a) and for the nonlinear analysis (b)

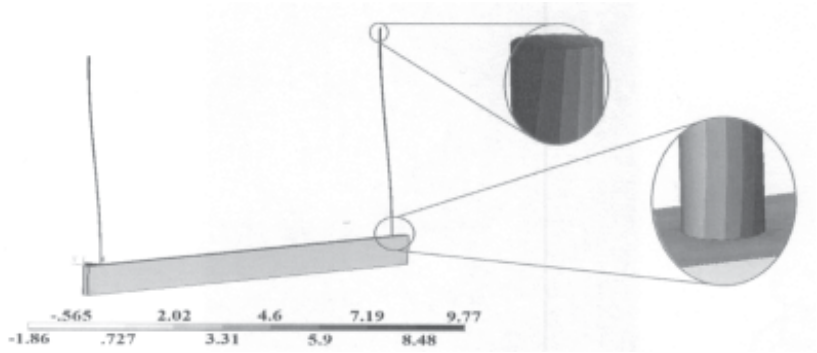

Fig. 10. Stress field σ_z [MPa] for the linear model

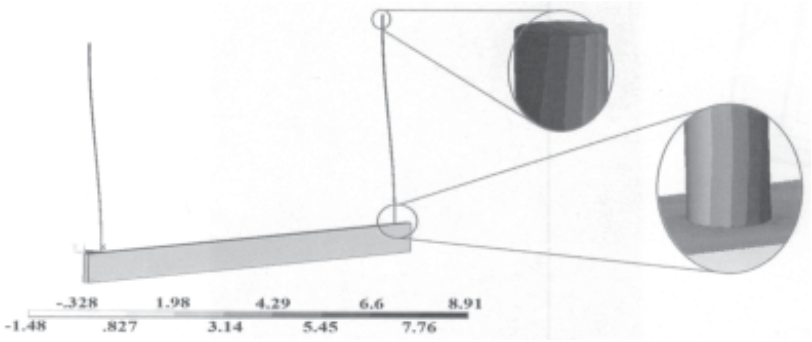

Fig. 11. Stress field σ_z [MPa] for the nonlinear model

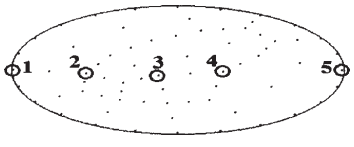

Fig. 12. Nodes in which the values of the stress σ_z were extracted

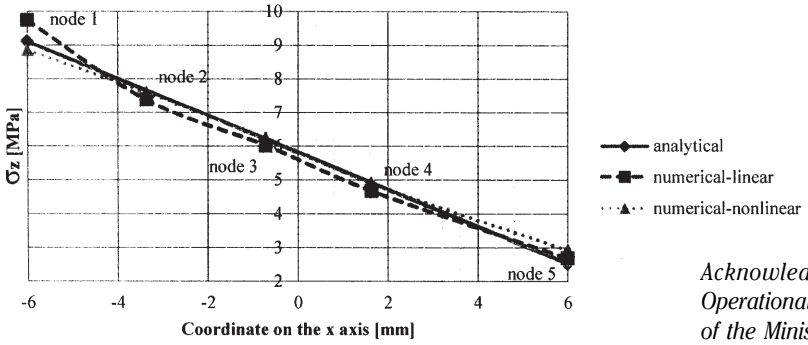

Fig. 13. Variation of the σ_z stress on the direction L-R in the three studied cases

The difference between the maximum stress obtained numerically with the linear and nonlinear model, is significant, due to the fact that the maximum stress is up to the point 4 from the schematized characteristic curve (fig. 8). The difference between the maximum stresses obtained with the two numerical models is:

$$E_\sigma = \frac{\left|\sigma_{max}^{linear} - \sigma_{max}^{non-linear}\right|}{\sigma_{max}^{non-linear}} \cdot 100 = \\ = \frac{|9.77 - 8.91|}{8.91} \cdot 100 = 9.65\%,$$

while the difference between the displacements at the lower end of the suspension element is even higher, having the value:

$$E_u = \frac{\left|u^{linear} - u^{non-linear}\right|}{\sigma^{non-linear}} \cdot 100 = \\ = \frac{|44.97 - 54.75|}{54.75} \cdot 100 = 17.86\%.$$

Conclusions

Taking into account the errors introduced in the numerical calculations by considering the material as linear it is necessary in such analyses to consider material non-linearity. Displacement values are important, because, as it was shown in the paper, they influence the efficiency of the sifting process.

The suspension elements of the SPP 420 plansifter can be manufactured from the material studied in this paper, since the maximum stresses are much lower than the ultimate strength of the material M5. The proposed calculation methodology can be adapted for other models of sifting machines and their suspension system. One should mention that, for a given motion amplitude of the analysed plansifter, any modification of the parameters used to calculate the bending stiffness of a suspension element leads to other values of the force with which the sieve acts on it. Also, one must take into account the number of supports, the weight of the plansifter and the maximum load during functioning. All these factors influence the values of loads, and, implicitly, the maximum stress.

The force with which the suspension system acts on the plansifter is important for the actuating mechanism in rotational motion. This may contribute to lower power consumption of the motor during movement. If the bending stresses are dangerous, another clamping system may be considered, in order to reduce or remove the bending, for example joint - joint. In this case, the force acting on the plansifter is eliminated.

One aspect that should be considered regarding the proposed material for manufacturing the suspension elements is the fatigue behaviour. The stress cycle is fully reversed and it has a period equal to the time in which a plansifter point describes a full circle in the horizontal plane. The study of the fatigue strength of the proposed biodegradable material is a further direction of research.

Acknowledgement: The work has been funded by the Sectoral Operational Programme Human Resources Development 2007-2013 of the Ministry of European Funds through the Financial Agreement POSDRU/159/1.5/S/134398.

References

1. RANKEN, M. D. (editor), Food Industries Manual, Springer Science & Business Media, 2012, page 193;
2. JANSEN, M., GLASTONBURY, J., The size separation of particles by screening, Powder Technology 1, pp. 334-343, 1967;
3. LIU, K.S., Some factors affecting sieving performance and efficiency, Powder Technology, Vol. 193, page 208-213, 2009;
4.*** http://www.selis.com.tr/default.asp?kategori= urungoster&uruncat=ogutme&dil=eng&urunid=28, accessed: 29.04.2015;
5.CONSTANTIN, G.A., Researches on the sifting and sorting process of grist fractions in an industrial milling plant, Doctoral thesis, "Politehnica" University of Bucharest, 2014;
6. STĂNESCU, M.M., BOLCU, D., CIUCĂ, I., DINIĂ, A., Non Uniformity of Composite Materials Reinforced with Carbon and Carbon-Kevlar Fibers Fabric, Mat. Plast., **51**, no. 4, 2014, p. 355
7. RAMESH, M., PALANIKUMAR, K., HEMACHANDRA REDDY, K., Comparative Evaluation on Properties of Hybrid Glass Fiber - Sisal/ Jute Reinforced Epoxy Composites. In: Procedia Engineering, 2013, Vol. 51, pp. 745-750;
8. SILVA, F.A., FILHO, R.D.T., FILHO, J.A.M., FAIRBAIRN, E.M.R., Physical and mechanical properties of durable sisal fiber-cement composites. In: Construction and Building Materials, 2010, Vol. 24, pp. 777-785;
9. ALOMAYRI, T., SHAIKH, F.U.A., LOW, I.M., Effect of fabric orientation on mechanical properties of cotton fabric reinforced geopolymer composites. In: Materials and Design, 2014, Vol. 57, pp. 360-365;
10. ALOMAYRI, T., SHAIKH, F.U.A., LOW, I.M., Synthesis and mechanical properties of cotton fabric reinforced geopolymer composites. In: Composites: Part B, 2014, Vol. 60, pp. 36-42;
11. GON, D., DAS, K., PAUL, P., MAITY, S., Jute composites as wood substitute. In: International Journal of Textile Science, 2012, Vol. 1, pp. 84-93
12. Pamuk, G., Ceken, F., Comparison of the mechanical behavior spacer knit cotton and flax fabric reinforced composites. In: Industria Textilă, 2013, vol. 64, issue 1, pp. 3-7;
13. MOHANTY, A. K., MISRA, M., DRZAL, L. T., Journal of Polymers and the Environment, 2002, Vol. 10, pp. 19-26;
14. GON, D., DAS, K., PAUL, P., MAITY, S., Jute composites as wood substitute. In: International Journal of Textile Science, 2012, Vol. 1, p. 84-93;
15. *** SR EN ISO 527-1 (2000) PLASTIC MATERIALS. Determination of tensile properties. Part 1: General principles;
16. CONSTANTIN, G.A., VOICU, GH., TUDOSE, V., PARASCHIV, G., IVANCU, B., Analysis of suspending system for plansifters from milling plants, Actual Tasks on Agricultural Engineering, 2015, Vol. 43, p. 495-
17. BUZDUGAN, GH., Rezistena materialelor (Strength of materials), Editura Tehnică, Bucuresti, 1980 (in Romanian);
18. RADES, M., Rezistena materialelor I (Strength of materials I), Editura Printech, Bucuresti, 2010 (in Romanian);
19. *** http://148.204.81.206/Ansys/150/ANSYS%20Mechanical%20Users%20Guide.pdf (ANSYS Mechanical user guide, 2013), accessed: 29.04.2015

Manuscript received: : 24.06.2015